*Eksplorium* *p*-ISSN 0854-1418
Volume 46 No. 2, June 2025: 255–269 *e*-ISSN 2503-426X

# Synthesis And Characterization of Nio /V2o5 /Ag2o Nanocomposites and Application in Dye-Sensitized Solar

Noor Mustafa Kamal[1], Amer Muosa Juda[2]

[1, 2]Department of Chemistry/ University of Kufa/ College of Science / Iraq.

Noorm.Muhsin@Uokufa.Edu.Iq

Article Received: 10 May 2025, Revised: 05 June 2025, Accepted: 15 June 2025

**Abstract:** In this study, a simple chemical method was used. A nanocomposite of nickel oxide and vanadium oxide was prepared, and silver oxide was added to this composite. The compounds were characterized using X-ray diffraction to show additional diffraction peaks in the spectrum of nickel oxide, vanadium oxide, and silver oxide for the second compound. Comparing these spectra with the spectrum of the oxides proved the correctness of the preparation of the compounds. The microstructure of the resulting compounds was examined via (FESEM). Differences between the synthesized compounds were also identified using FE-SEM, TEM, AFM, BET, and FTIR techniques. The prepared nanoparticles were used as electrodes in solar cells using a natural dye (green). The results showed that the efficiency of the prepared nanocatalyst NiO/ $V_2O_5$, was higher than that of the catalyst NiO/ $V_2O_5$ /Ag2O , as calculated by the conversion efficiency (η) of the cells under study. This is due to several factors, including the energy gap and the difference in surface area

**Keywords:** NiO/ $V_2O_5$ nanocomposites, NiO/ $V_2O_5$ /Ag2O nanocomposites, Co-precipitation, Dye-Sensitized Solar.

## INTRODUCTION

In topical times, the rapid progression of nanotechnology has prompted a substantial change in several work uses. [1]. The unique properties of nanomaterials, as well as improved mechanical, chemical, optical, thermal, and electrical performance, consume attracted considerable attention since scientists in several fields.[2] . Commercial uses of nanomaterials are growing in purchaser products, such as grease paints, food crops, electronics, automotive, and more. Nanotechnology applications have spread across various productions, as well as biotechnology, creation, renewable energy, and healthcare. Moreover, nanotechnology proposes solutions to eco-friendly problems, particularly in certain areas. Dye-sensitized solar cells.[3, 4]Photovoltaic technology (PV) is considered one of the greatest capable innovations because it can transform solar energy into electrical energy. The Sooq increasingly concentrates on dye-sensitized solar cells within the various photovoltaic technologies. [5] Photovoltaic cells are also semiconductor strategies. (PV) transform sunlight, encompassing visible light, ultraviolet, and infrared energy, in to direct current (DC) by means of the photovoltaic conclusion **[6]** One of the most generally used solar energy systems currently is photovoltaic (PV) solar technology, which is powered by light, operates at temperatures close to room temperature, and contains no moving components. Furthermore, solar energy is an unlimited and completely permitted supply. [7].Dye-enhanced solar cells are a third-generation solar cell technology[8]. the cells are manufactured using a sensitive dye deposited on a nanocrystalline sheet. The dye particles absorb photons, convert enthusiastic, and statement enthusiastic electrons into the semiconductor's conduction band, producing electrical power[9]. The dyes used are confidential as natural and synthetic. The main advantages of DSCs contain low production costs, ease of fabrication, and being a cost-effective and biologically workable other to other solar energy technologies. The first DSCs were introduced by O'Regan and Grätzel in

1991[10] as a potential another to conventional solar cells. These cells are translucent, easy to manufacture, and economical, as the materials used in their production are relatively low-cost [11]. The fundamental characteristics required for effective dyes in dye-sensitized solar cell requests are: The dye must absorb light across the visible and near-infrared spectra. The dye must exhibit a substantial affinity for the metal oxides that will be adsorbed onto the semiconductor sheet. The energy levels of the dye must align with those of the metal oxide and electrolyte. The dye's LUMO exceeds the conduction band of the metal oxide, whereas the dye's HOMO surpasses the HOMO of the electrolyte., [10] Inhibit dye aggregation to reduce the nonradiative transition from the excited state to the ground state. The dye must demonstrate chemical, thermal, and photostability over a protracted period, which currently represents the primary barrier to commercialization.[12, 13]**.**

## MATRIALS

All materials, nickel(II) chloride hexahydrate ($NiCl_2·6H_2O$, 99%), sodium hydroxide (NaOH, 97%), Cetyltrimethyl Ammonium Bromide (CtAB , 99% purity ), Sodium metavanadate (NaVO3 , 99% purity ) Silver nitrate ($AgNO_3$, 99% purity), and Polyvinylpyrrolidone (PVP, 98%) were got from Merck (Germany). Very solutions were prepared using deionized (DI) water.

## PROCDUR

### PREPARATION OF NiO/V2O5 NANOCOMPOSITe BY CO-PRECIPITATION

NiO/V2O5 nanocomposite was prepared using co-precipitation techniques. The stoichiometric molar ratios of 1:1 were used as follows: The first step was to add 1.949 gm of $NiCl_2.6H_2O$ to 200 cm3 of deionized water. 0.8 gm/ml NaOH was then added to the solution, resultant in a concluding pH of 8–9, under magnetic stirring for 40 min at 50 °C. [10]. After, 1.2 gm of sodium metavanadate was dissolved completely, followed by adding 2.4 g of ammonium chloride to the solution after 3 minutes until it was completely dissolved. Later, at 10 mint , 0.6 gm of CtAB was added to the solution, and the blend temperature was increased to 80 °C for three hours. [11], The solutions were mixed below magnetic stirring used for 60 min at room temperature. In the ending step, they were rinsed with distilled water and ethanol three times to remove reaction byproducts and dried at 70°C for 10 h. The dried samples were then calcined at 600°C for 30 mint to obtain nickel oxide/vanadium oxide composite nanoparticles.

### PREPARATION OF NiO/V2O5/ $Ag_2O$ NANOCOMPOSITe BY CO-PRECIPITATION

$NiO/V_2O_3/Ag_2O$ compounds were produced by co-precipitation at a molar ratio of 1:1:1: In the first step, 0.5 g of $NiO/V_2O5$was added to 100 $cm^3$ of deionized water, 0.5 g of PVP was additional to the mixture, then magnetically moved used for 5 min at apartment temperature. Next, 1.393 g of $AgNO_3$ was added, and the final pH was adjusted to 8-9 via adding 0.8 M NaOH. The mixture was magnetically stirred for 30 mint. and then left unstirred for 15 minutes. In the final step, it was washed with distilled water and ethanol three times to eliminate excess water and dried at 60 °C for seven hours [14].

**SYNTHESIS DYE SENSITIZED SOLAR CELL .**

Solar cells were prepared from the prepared compounds using fluorine tin oxide (FTO) films with a natural dye, using the following steps:

**PREPARE REDOX ELECTROLYTES BETWEEN TWO ELECTRODE:** KCl (100 g. L-1): 10 grams of pure KCl was dissolved in 100 mL of DIW , To prepare 0.1 M solution of iodine ,10 gm of potassium iodide (KI) was dissolved in 25 mL of DIW, and 3.175 g of iodine (I2) was additional until dissolved. Then the solution was diluted and prepared in 250mL and the solution is kept [15]

**EXTRACTION OF NATURAL DYE :** it was prepared by cutting the radish leaves and washing it well ,then preparing the dye solution with an electric blender filtering the solution, and storing it in a dark bottle show Figure 1


Figure 1. Extraction of natural dye

**PREPARE THE ANODE ELECTRODES**: Sensitized solar cells are prepared as follows: The anode electrode of the FIO-type solar cells is prepared. A minimal amount of the prepared nanomaterial (0.137-0.307) g is taken, mixed with an ethanol mixture, and placed on the surface of the solar cell, leaving the edges of the cell uncovered by the nomaterial. The electrode is left to dry completely after being sited in an oven at 60°C. The anode electrode is then immersed in a green dye solution attached to the nano-surface for 24 hours in the dark. Afterwards, the solar cell is removed and dried in the dark. The anode electrode is also dried. This process is applied to all prepared nanomaterials.

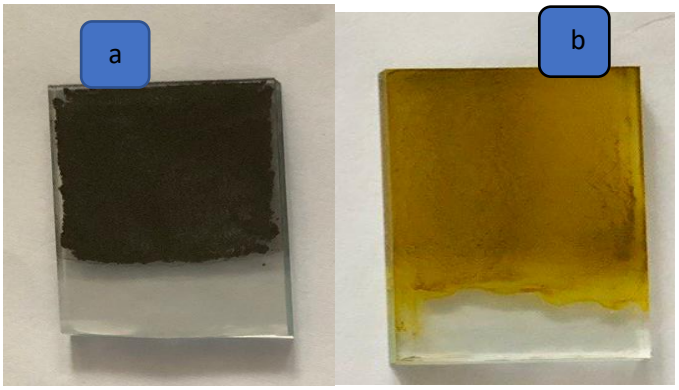


Figure 2. immerge working electrode in dye solution .(a) NiO/$V_2$ $O_3$/$Ag_2O$ nanocomposites (b) NiO/$V_2O_3$ nanocomposites

**PREPARE THE CATHODE ELECTRODES .**

The cathode electrodes is prepared by covering the surface of the solar cell type ( FTO) with carbon ( Graphite ) , leaving the edges also on the solar cell. So the cathode electrode was equipped**,**

The final step is to calculate the power conversion efficiency (η) of the prepared DSSC cell based on the current density-voltage (J-V) characteristic of the cell exploitation a Keithley 2400 (Figure 2-6). A light intensity of less than 22.53 mW/cm2 from a 125 W xenon lamp was measured as per a source. Dye-sensitized solar cells were prepared by depositing the prepared nanomaterials (NiO,/V2O5, NiO /V2O5/Ag2O) on the surface of an FTO wafer. After drying, the cells were immersed in a natural green dye (radish leaf) as the positive electrode, while graphite was using as the negative electrode. Furthermore, an iodine/iodide solution was prepared for use as a conducting electrolyte using a 0.1 M iodine solution. Figures 3 show how a solar cell works and what it looks like after measuring its efficiency with a Keithly.

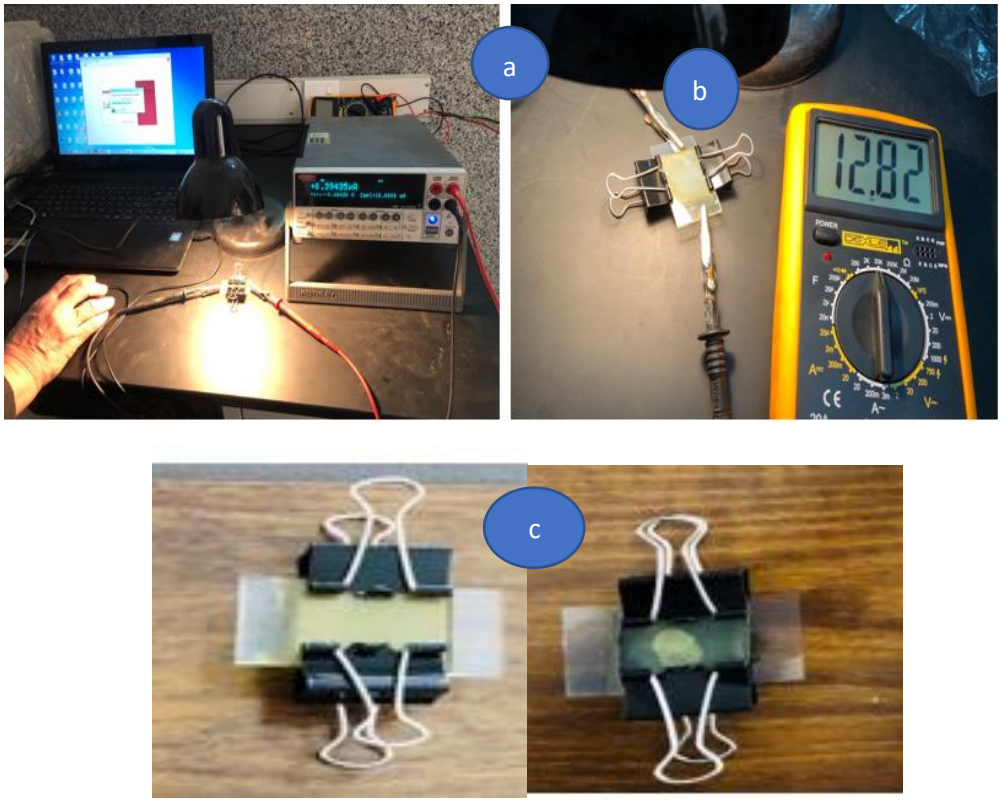


Figure 3. (a)(b) Keithley 2400 Series SourceMeter , ( c)show how the solar cell woks and shapes after measuring efficiency with the Keithly device ( The final form of DSSCs.) .

## RESULTS AND DISCUSSIONS

### 1.XRD ANALYSIS

X-ray diffraction (XRD) analysis of the nickel oxide/vanadium oxide nanocomposite was performed, show in Figure 4. The figure shows that the characteristic peaks indexed to nickel oxide (03-065-6920) correspond to 2θ values of 37.225°, 43.268°, 62.875°, 75.420°, and 79.50°, which are associated with the millier planes (001), (200), (111), (021), and (002), respectively, with a space group of C2/m. The preferred orientation along the (200) plane is observed. The XRD spectra of V2O5 burned at 600 °C (Fig. 2) reveal peaks at 2θ = 25.20° (102) and 33.73° (212), along with additional peaks at 2θ = 15.42°, 20.31°, 26.19°, 31.07°, 34.30°, 45°, and 51°, which correspond to the (200), (001), (110), (301), (310), (411), and (002) millilitre planes, corresponding to ICDD card numbers [03-065-6920] and [00-041-1426], respectively **[16, 17] .** There are some slight shifts in the positions of nickel and vanadium oxide peaks, along with the appearance of additional peaks due to the overlapping contributions between the two oxides or the possible formation of intermetallic compounds. Such structural modifications can enhance the physical and chemical properties of the material, counting increasing the surface area and improving the kinetics of ion release **[18] .** Debye–Scherrer equation [19]. the size crystal of the resulting models was assigned a crystal size between (6-26) nm for nickel oxide/vanadium oxide nanoparticles per an average size of (13.4) nanometers.

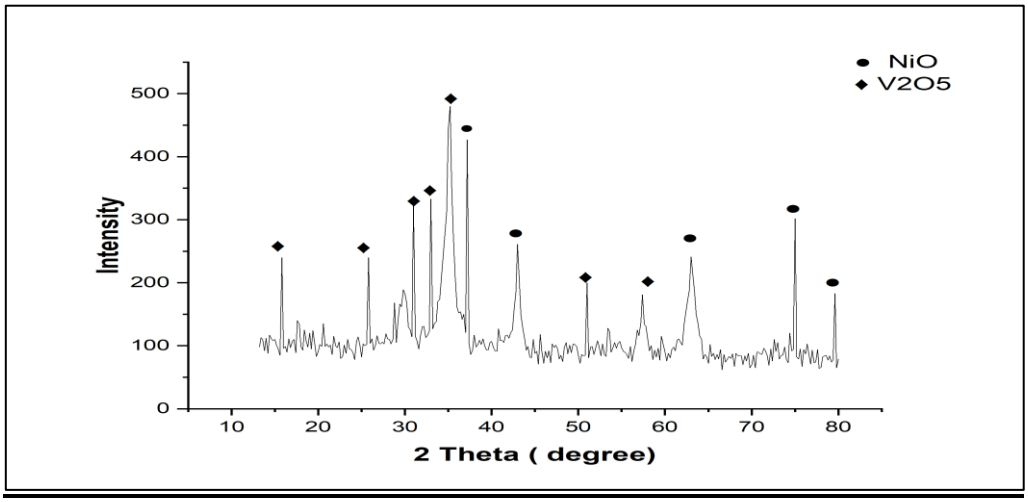


Figure 4. X-ray diffraction patterns of NiO / V2O5 composite

The structural composition and phase purity of the NiO/V2O5/Ag2O composite were examined at ambient temperature with X-ray diffraction (XRD), and the peaks of silver oxide nanoparticles (JCPDS card No. 76-1393)[14, 16] , seen in Figure 5. utilising various ratios of NiO and V2O5 to Ag2O ( 1:1:1) .The NiO/V2O5/Ag2O composite exhibits peaks corresponding to each component (NiO, V2O5, and Ag2O), clearly delineating the composite's composition. The diffraction pattern ( X-ray ) of the nanocrystals indicates that the synthesised nanoparticles demonstrate a reduced level of crystallinity in comparison to the nanocrystals of both NiO/V2O5/Ag2O composites[20].

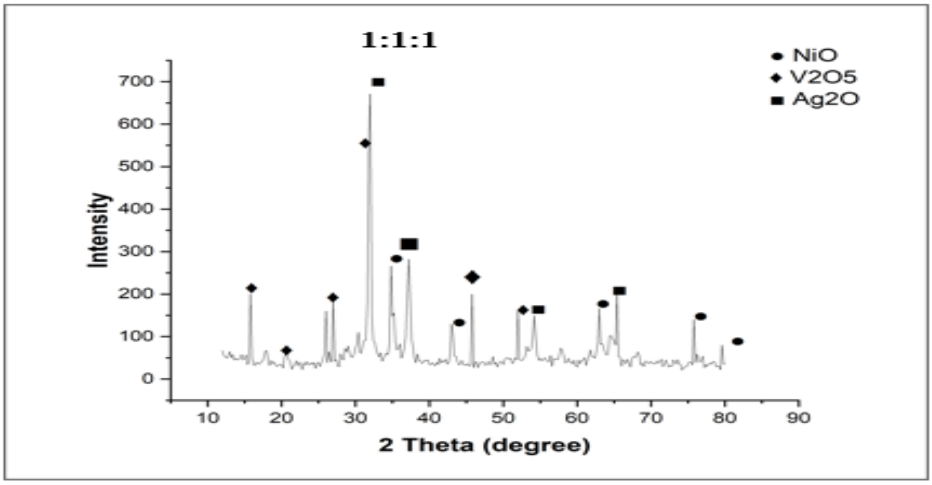


Figure 5. X-ray diffraction patterns **of** NiO/V2O5/ Ag2O composite.

The structure crystal of the produced illustrations ( 1:1:1 ) was determined by means of the Scherrer equation crystallite size of nickel oxide - vanadium oxide - silver oxide composite between (5-19), and average is (9.85) nm.

## 2. FESEM ANALYSIS

The SEM gives the magnified images of the size, shape, composition, crystallography, and other physical and chemical properties of a specimen. Surfaces are magnified in a scanning electron microscope several whiles to interpretation surface structures and evaluate surface variations [21] FESEM image 6 shows a broad distribution of particles on the sample surface. These images show that the particles are clustered into small aggregates (clusters) without forming large agglomerates, indicating a relatively stable nanostructure. The contrast in shadows and light intensity between the two composite images indicates a difference, supporting the hypothesis of a surface-active nanocomposite formation , The FESEM images also support that the prepared composite is characterized by good nano distribution, a quasi-spherical structure, and moderate porosity, making it suitable for applications.

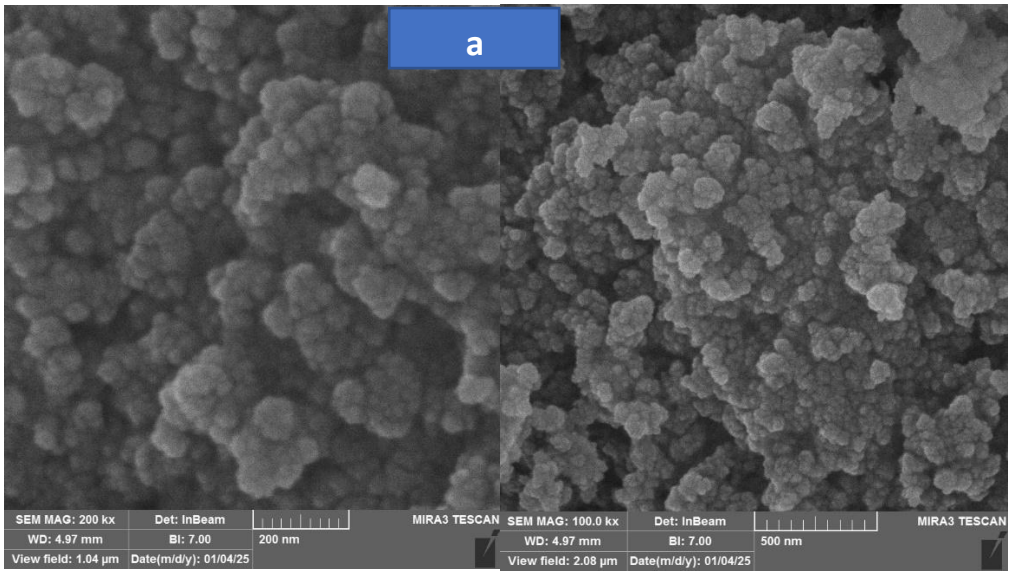

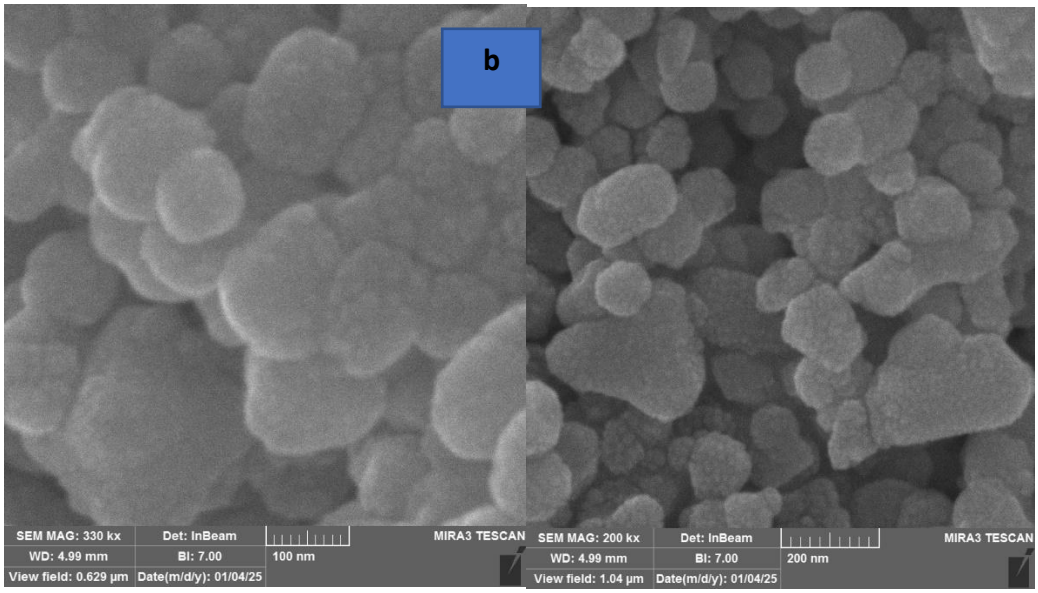


Figure 6 FESEM micrograph images of (a) NiO/ $V_2O_5$ nanocomposites (b) NiO/ $V_2O_5$ / Ag2O nanocomposites

### 3-TEM ANALYSIS

Transmission electron microscopy is one of the most widely used microscopic techniques to provide information about the topography, shape, contrast, form, size, composition, and crystallinity of a sample[22] In Figure 7 a , the transmission electron microscope image shows that the nanoparticles take the form of sheets arranged in dense clusters. Figure 7 b shows variation in nanoscale morphology, and some high-contrast regions are attributed to the higher electron density silver nanoparticles, which were likely deposited on the surface or within the n-composite, indicating a physical complex between the two materials. This structural diversity indicates the flexibility of the resulting nanostructure and the influence of preparation conditions on particle shape and distribution [23].

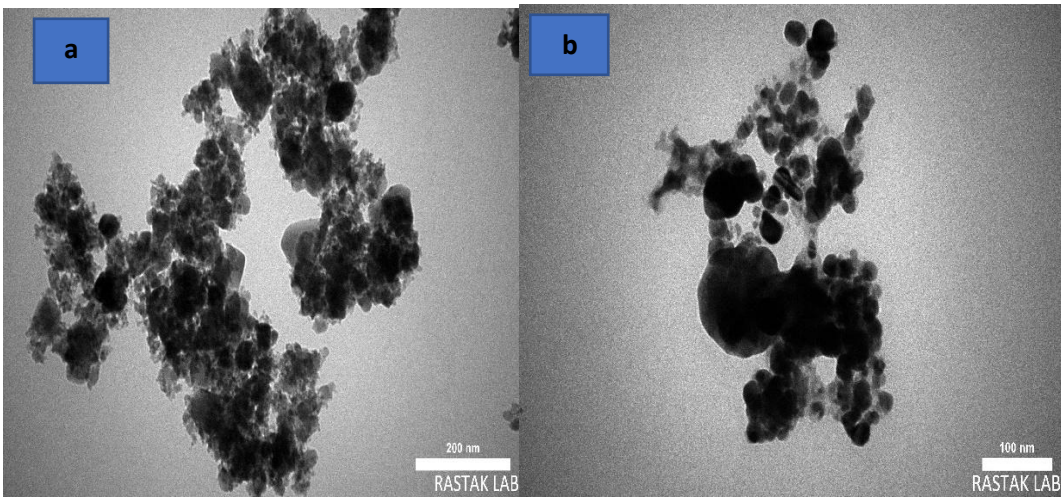


Figures7. TEM micrograph images of (a) NiO / $V_2O_5$ (b) NiO / $V_2O_5$ / Ag2O

### 4.AFM ANALYSIS

Topographical imaging with an atomic force microscope (AFM) is an efficient technique for acquiring detailed information regarding the morphology, topography, and composition of diverse surfaces. In AFM images, opaque colours indicate weak structures, while bright colours signify elevated structures, owing to the various trajectories of grain particles. The AFM measurements yield precise data regarding the size distribution, average nanoparticle diameter, and surface homogeneity of nanoparticles. Figure 8 , displays in the 3D image a fiber with strong vertical arrangement and variable degrees of surface homogeneity, and illustrates the distribution of the nickel oxide - vanadium oxide , the nickel oxide- vanadium oxide- silver oxide nano composite.

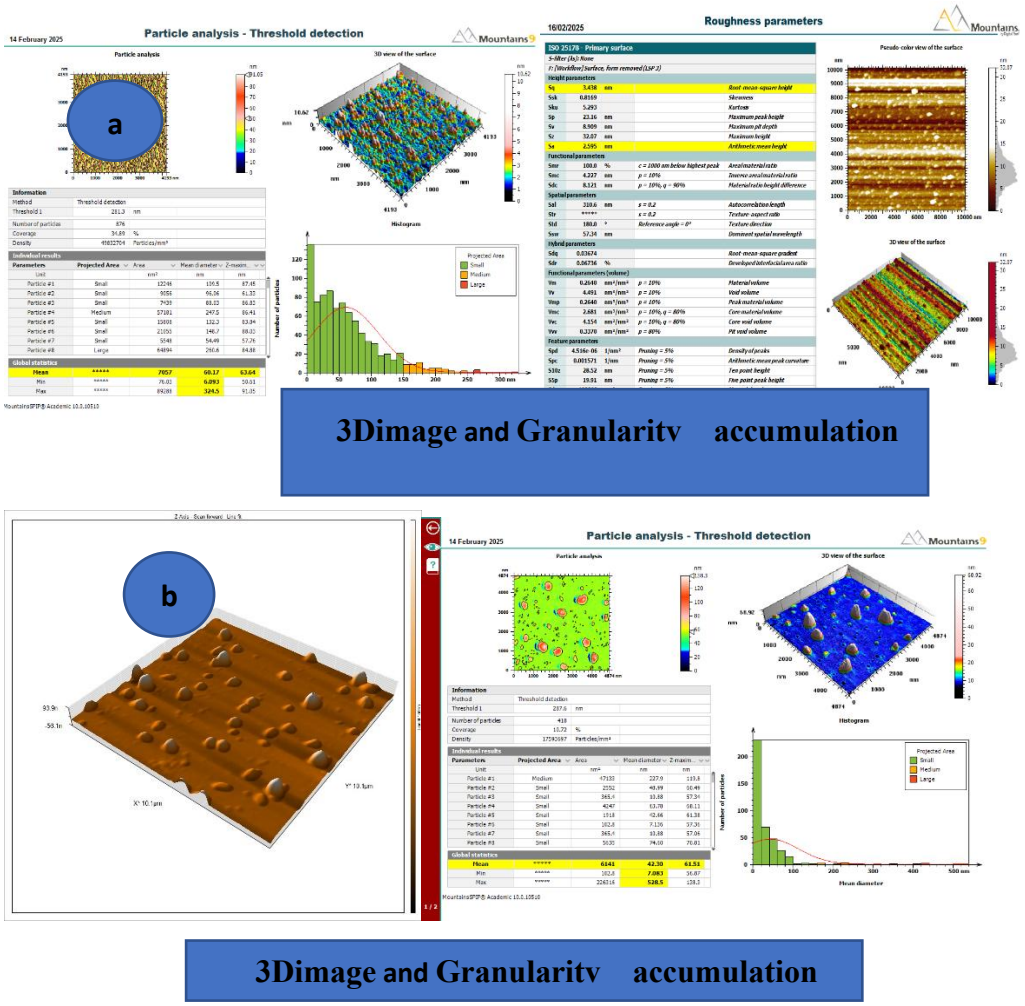


Fig. 8. AFM of (a) nickel oxide / vanadium oxide nano composite, (b) nickel oxide / vanadium oxide/ silver oxide nano composite

## 5- BRUNAUER-EMMETT-TELLERS SPECIFIC SURFACE AREA (BET) ANALYSIS:

The Brunauer-Emmett-Teller (BET) method is usually used to compute the specific surface area based on nitrogen adsorption isotherm measurements at 77 K . [24] Data are typically used in the relative pressure range of 0.05 to 0.3 [25]. the surface area of (NiO/ V2O5, and NiO/ V2O5/Ag2O) by adsorbing nitrogen gas at (-196°C) by the surface. BET method measures the volume of gas (usually nitrogen) adsorbed on a solid surface at different relative

pressures (P/P0), where P is the gas pressure, and P0 is the saturated vapour pressure. This data is plotted as an adsorption isotherm, a graph of the amount of gas adsorbed versus the relative pressure. The grades are listed in Table 1, which shows the surface area and the total pore size in the table below for all the prepared nanoparticles and compounds. The increase in the surface area leads to higher efficiency in the work of solar cells [26].

Table 1 The characteristic surface of the nanoparticle and nanocomposites in the BET method**.**

| **Compound** | **surface area** | | |
|---|---|---|---|
| | Surface are $m^2/g$ | Total pore volume ($p/p_o$ =0.95)$cm^3/g$ | Mean pore diameter nm |
| NiO/V2O5 | 72.324 | 0.307840 | 17.02540 |
| NiO/V2O5/Ag2O | 1.7395 | 0.0143598 | 3030.1993 |

## 6- FTIR SPECTRA

As exposed in Figure 9. The fourier transform infrared spectroscopy is a proficient practice used for the qualitative identification of organic constituents.[27, 28] . FTIR spectra of the synthesised nickel oxide and vanadium oxide composite (1:1) were obtained within the range of 350 to 4000 cm-1; the 3412.08, 1635, and 1319 cm-1 may result from the stretching and bending vibrations of -OH adsorbed on the catalyst surface from the environment during Fourier transform infrared examination and Generally appears around 1365 $cm^{-1}$. In aromatic nitro compounds, this band also shifts lower, to 1360-1290 $cm^{-}$ [27, 29, 30]. Moreover, The vibrational peaks at 950–1030 $cm^2$ are ascribed to the stretching vibration of the terminal V=O bond. The peaks seen at 780–850 $cm^2$ signify the asymmetric stretching vibration of the V–O–V bond, while the 530–580 $cm^2$ range corresponds to the symmetric stretching vibration of the V–O–V bond. The peak at 1651 $cm^2$ corresponds to vibrational frequencies linked to the O–H bond of the water molecule. The 2800 to 3000 $cm^2$ region exhibits both asymmetric and symmetric stretching vibrations of the CH2 and CH3 groups. The band at 1460 $cm^2$ results from the asymmetric stretching vibrations of the CH2 and CH3 groups [28]. This confirms the formation of the composter NiO-V2O5.

Fourier transform infrared (FTIR) spectroscopy was performed to confirm the company of nickel oxide, vanadium oxide, and silver oxide nanoparticles as prepared. As shown in Figure 9, the spectra clearly show absorption bands corresponding to nickel oxide, vanadium oxide, and silver oxide complexes, consistent with previous research. [28, 31, 32]

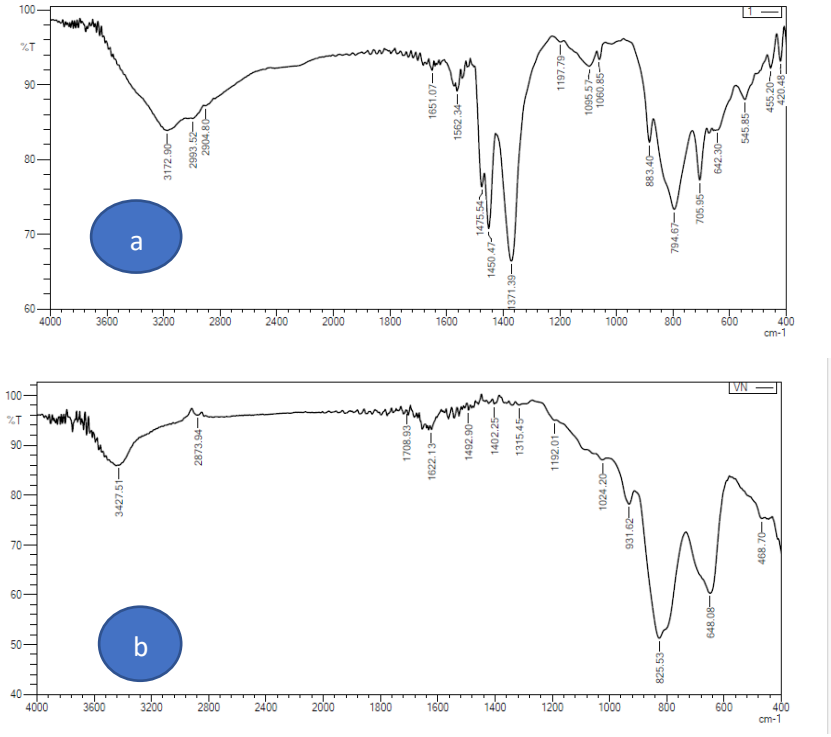


Figure 9. FTIR spectrum of (a) NiO/V2O5 Composite , (b) NiO/V2O5/ Ag2O composites.

## DIFFUSE REFLECTANCE SPECTRA ANALYSIS (DRS )

The films' UV-Vis diffuse reflectance (DRS) spectra at room temperature were taken to estimate the optical band gap of the gained films, and these figures were functional to the Kubelka-Munk role.[33]. The Kubelka-Munk typical is one of the greatest widely used systems for estimating the intermediate optical band of dust trials or opaque films. In this typical, parts of the scattered reflection spectrum R are used. Finally, the R spectra of all the films found are on apartment temperature and contain a BaSO4 pollutant as a reference. The resulting relationship determines the band gap (for example).[34]. Regulate the photosensitive band gap energy (Eg) since DRS extents using the K-M role as a substitute of the "absorption coefficient" in the "Tauc relation " **[35]**. Show Figure 10 , Figure 11 .

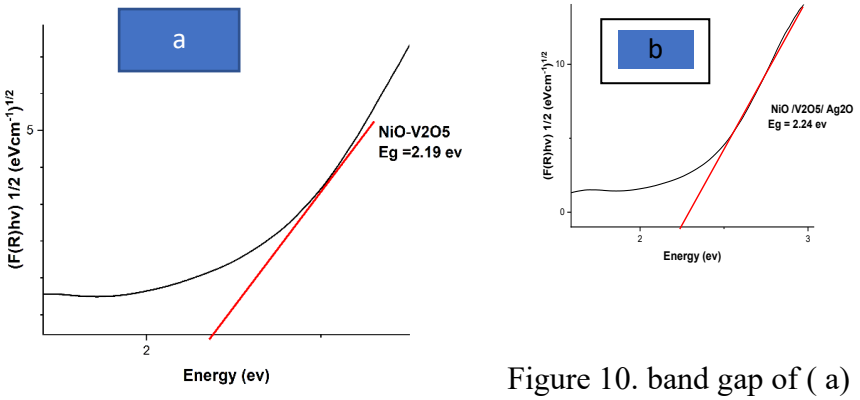


(b)

Figure 10. band gap of ( a) NiO /V2O5 and NiO /$V_2O_5$/ $Ag_2O$.

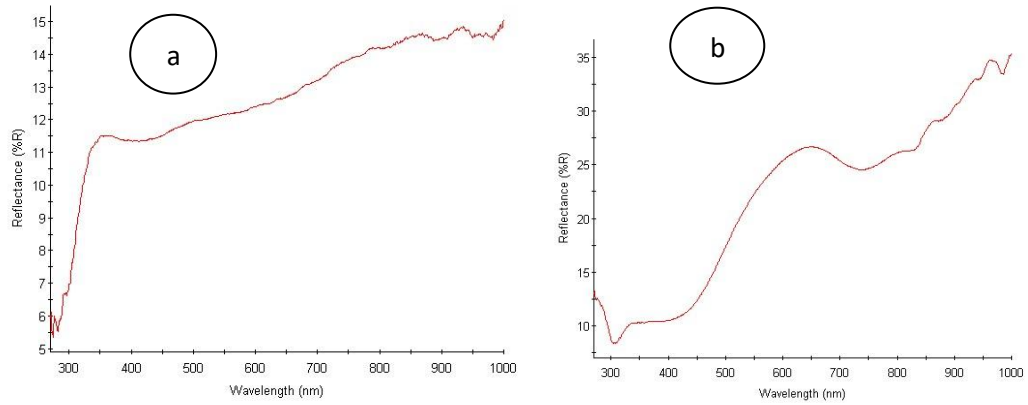


Figure 11. The diffuse reflectance spectra of (a) NiO/V2O5 , (b) NiO / $V_2O_5$/ $Ag_2O$

Table 2. the Energy band gab of the as-synthesized nanoparticles

| Compound nanoparticles. | Energy band gab Eg ( ev) in the study |
|---|---|
| NiO/V2O5 | 2.19 |
| NiO/V2O5/Ag2O | 2.24 |

The physical I-V diagram of dye-enhanced solar cells using natural dye is shown. Figures 12 provide data on the solar cell efficienc [36]. The power conversion efficiency (PCE) of the manufactured cells under study can be calculated by knowing both the current and voltage from the graph, where Jmax represents the maximum current density, Vmax represents the maximum voltage, Jsc represents the short-circuit current, and Voc represents the open-circuit voltage, using equation. (2)

$$\eta = Jsc.\ Voc.\ F / Pin.100\% \quad [36].$$

The results can be observed indicated that the efficiency of the solar cell dyed using natural dye gave NiO/V2O5 nanocomposite the highest efficiency of NiO/V2O5/Ag2O nanocomposites through the conversion efficiency value (η), as shown in Table 3 There are several reasons, including the difference in surface areas between nanomaterials and others, as each material has a larger surface area the, greater the dye adsorption capacity, as shown in Table (2). It can also be concluded that increas the surface area will enhance the dye adsorption on the nano surfaces. Also, the lower the gap energy, the higher the cell efficiency, and thus, increase the efficiency of dyed solar cells depends on the nature of the material and its physical properties. [37, 38].

Natural dyes are less effective than chemical dyes as they consume a slimmer absorption range, higher redox potentials, more rapid operating life, higher electron re-combination charges, and changed molecular structures[39] .

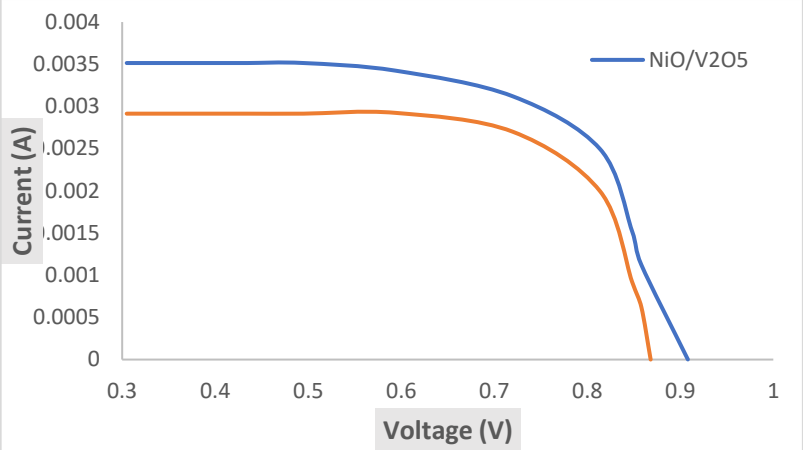


Figure 12. I-V Characteristics of prepared DSSCs natural dye

Table 3 Conversion efficiency value of the nanocomposites under study.

| Catalyst | Type of dye | (PEC) Isc(A) | Voc(V) | I(max) | V(max) | P(max) | FF | η% |
|---|---|---|---|---|---|---|---|---|
| NiO/V2O5 | natural | 0.000352 | 0.9072 | 0.00287 | 0.7538 | 0.00216341 | 6.7747352 | 0.002163406 |
| NiO/V2O5/Ag2O | natural | 0.00292 | 0.8691 | 0.00243 | 0.7565 | 0.0018383 | 0.72437358 | 0.001838295 |

## CONCLUSION

NiO / $V_2O_5$and NiO / $V_2O_5$/$Ag_2O$ nanocomposites are prepared by a simple, safe, economic, and chemical precipitation method. The molecular formula, structural, topographic, morphologic, and electro-optical analytical characterization of electrochemically prepared NiO / $V_2O_5$and NiO / $V_2O_5$/$Ag_2O$ nanocomposites were successfully studied using a change of specialized techniques, by FTIR, XRD, DRS , FESEM, TEM, and AFM.the efficiency of the solar cell dyed via natural dye gave NiO/V2O5 nanocomposite the highest efficiency of NiO/V2O5/Ag2O nanocomposites through the conversion efficiency value The prepared DSSC from NiO – $V_2O_5$ nanocomposite has better efficiency than the other nanoparticles NiO / $V_2O_5$/ $Ag_2O$ because the NiO / $V_2O_5$ nanocomposite has less band gap than NiO /$V_2O_5$/ $Ag_2O$ .

## ACKNOWLEDGMENT

The opportunity to work in the laboratory during this work was made possible by the personnel of the Graduate Studies Laboratory at the Chemistry Department, College of Science, University of Kufa, for which the authors are truly grateful.

**REFERENCES**

1. Findik, F.J.P.o.E. and N. Sciences, *Nanomaterials and their applications.* 2021. **9**(3): p. 62-75.
2. Yang, Z., et al., *Carbon nanotube-and graphene-based nanomaterials and applications in high-voltage supercapacitor: A review.* 2019. **141**: p. 467-480.
3. Kumar, A., et al., *Highly visible active Ag2CrO4/Ag/BiFeO3@ RGO nano-junction for photoreduction of CO2 and photocatalytic removal of ciprofloxacin and bromate ions: The triggering effect of Ag and RGO.* 2019. **370**: p. 148-165.
4. Mohammed, E.M.M., *Composite Nanostructured Materials for Renewable Energy Applications*. 2023, Linkopings Universitet (Sweden).
5. Agrawal, A., et al., *Advancements, frontiers and analysis of metal oxide semiconductor, dye, electrolyte and counter electrode of dye sensitized solar cell.* 2022. **233**: p. 378-407.
6. Hasan, M., et al., *Harnessing solar power: a review of photovoltaic innovations, solar thermal systems, and the dawn of energy storage solutions.* 2023. **16**(18): p. 6456.
7. Abdulhussein, S.F., S.M. Abdalhadi, and H.D.J.E.J.o.C. Hanoon, *Synthesis of new imidazole derivatives dyes and application in dye sensitized solar cells supported by DFT.* 2022. **65**(9): p. 211-217.
8. Chukwuemeka, E.J., et al., *Performance and stability evaluation of low-cost inorganic methyl ammonium lead iodide (CH3NH3PbI3) perovskite solar cells enhanced with natural dyes from cashew and mango leaves.* Adv. J. Chem. Sect. A, 2024. **7**(1): p. 27-40.
9. Wang, Z., et al., *Efficiency accreditation and testing protocols for particulate photocatalysts toward solar fuel production.* Joule, 2021. **5**(2): p. 344-359.
10. Jilakian, M. and T.H. Ghaddar, *Eco-friendly aqueous dye-sensitized solar cell with a copper (I/II) electrolyte system: efficient performance under ambient light conditions.* ACS Applied Energy Materials :(1)5 .2022 ,p. 257-265.
11. Maldon, B. and N.J.M. Thamwattana, *A fractional diffusion model for dye-sensitized solar cells.* 2020. **25**(13): p. 2966.
12. Semalti, P., S.N.J.J.o.n. Sharma, and nanotechnology, *Dye sensitized solar cells (DSSCs) electrolytes and natural photo-sensitizers: a review.* 2020. **20**(6): p. 3647-3658.
13. Devadiga, D., et al., *Dye-sensitized solar cell for indoor applications: a mini-review.* 2021. **50**: p. 3187-3206.
14. Xu, L., et al., *Flower-like ZnO-Ag 2 O composites: precipitation synthesis and photocatalytic activity.* Nanoscale research letters, 2013. **8**: p. 1-7.
15. Atrak, K., A. Ramazani, and S. Taghavi Fardood, *Green synthesis of amorphous and gamma aluminum oxide nanoparticles by tragacanth gel and comparison of their photocatalytic activity for the degradation of organic dyes.* Journal of Materials Science: Materials in Electronics, 2018. **29**: p. 8347-8353.

16. Govindarajan, D., V. Uma Shankar, and R. Gopalakrishnan, *Supercapacitor behavior and characterization of RGO anchored V 2 O 5 nanorods.* Journal of Materials Science: Materials in Electronics, 2019. **30**: p. 16142-16155.
17. Mousavi, M., S. Tabatabai Yazdi, and G. Khorrami, *Structural, Optical and Magnetic Characterization of Vanadium Pentoxide Nanoparticles Synthesized in a Gelatin Medium.* Journal of Nanostructures, 2021. **11**(1): p. 105-113.
18. Ramadan, R., *Enhancement the physical properties of V2O5/Ni0. 1Fe2. 9O4 nanocomposite.* Journal of the Australian Ceramic Society, 2024. **60**(5): p. 1437-1446.
19. Gholami-Shabani, M., et al., *Mycosynthesis and Physicochemical Characterization of Vanadium Oxide Nanoparticles Using the Cell-Free Filtrate of Fusarium oxysporum and Evaluation of Their Cytotoxic and Antifungal Activities.* Journal of Nanomaterials, 2021. **2021**(1): p. 7532660.
20. Shalaby, N.H., et al., *Waste-extracted Zn and Ag co-doped spent catalyst-extracted V2O5 for photocatalytic degradation of Congo red dye: effect of metal-nonmetal co-doping.* Catalysts, 2023. **13**(3): p. 584.
21. Ural, N., *The significance of scanning electron microscopy (SEM) analysis on the microstructure of improved clay: An overview.* Open Geosciences, 2021. **13**(1): p. 197-218.
22. Shume, W.M., H.A. Murthy, and E.A. Zereffa, *A review on synthesis and characterization of Ag2O nanoparticles for photocatalytic applications.* Journal of chemistry, 2020. **2020**(1): p. 5039479.
23. Wang, J., et al., *Hydrothermal preparation of porous NiO nanoflake arrays@ V2O5 nanoparticles composite for high performance supercapacitive electrode material.* Journal of Alloys and Compounds, 2024. **976**: p. 172955.
24. Mohan, V.B., K. Jayaraman, and D. Bhattacharyya, *Brunauer–Emmett–Teller (BET) specific surface area analysis of different graphene materials: a comparison to their structural regularity and electrical properties.* Solid State Communications, 2020. **320**: p. 114004.
25. Shimizu, S. and N. Matubayasi, *Surface area estimation: Replacing the Brunauer–Emmett–Teller model with the statistical thermodynamic fluctuation theory.* Langmuir, 2022. **38**(26): p. 7989-8002.
26. Wu, T., et al., *Lead-free tin perovskite solar cells.* Joule, 2021. **5**(4): p. 863-886.
27. Moavi, J., F. Buazar, and M.H. Sayahi, *Algal magnetic nickel oxide nanocatalyst in accelerated synthesis of pyridopyrimidine derivatives.* Scientific reports, 2021. **11**(1): p. 6296.
28. ayalakshmi, T., R. Harini, and G. Nagaraju, *Lithium ion battery performance of micro and nano-size V2O5 cathode materials.* Materials Today: Proceedings, 2022. **65**: p. 200-206.
29. Khairnar, S.D. and V.S. Shrivastava, *Facile synthesis of nickel oxide nanoparticles for the degradation of Methylene blue and Rhodamine B dye: a comparative study.* Journal of Taibah University for Science, 2019. **13**(1): p. 1108-1118.

30. Saravanakkumar, D., et al., *Synthesis of NiO doped ZnO/MWCNT Nanocomposite and its charecterization for photocatalytic & antimicrobial applications.* J. Appl. Phys, 2018. **10**(3): p. 73-83.
31. Moavi, J., F. Buazar, and M. Sayahi, *Algal magnetic nickel oxide nanocatalyst in accelerated synthesis of pyridopyrimidine derivatives. Sci Rep 11: 629*.2021 .6
32. Vinay, S., et al., *Facile combustion synthesis of Ag2O nanoparticles using cantaloupe seeds and their multidisciplinary applications.* Applied Organometallic Chemistry, 2020. **34**(10): p. e5830.
33. Parveen, S., et al., *Iron/vanadium co-doped tungsten oxide nanostructures anchored on graphitic carbon nitride sheets (FeV-WO 3@ gC 3 N 4) as a cost-effective novel electrode material for advanced supercapacitor applications.* RSC advances, 2023. **13**(38): p. 26822-26838.
34. Caglar, Y., S. Ilican, and M. Caglar, *FESEM, XRD and DRS studies of electrochemically deposited boron doped ZnO films.* Mater. Sci. Poland, 2017. **35**(4): p. 824-829.
35. Alkallas, F., K. Elshokrofy, and S. Mansour, *Structural and diffuse reflectance characterization of cobalt-doped titanium dioxide nanostructured powder prepared via facile sonochemical hydrolysis technique.* Nanomaterials and Nanotechnology, 2019. **9**: p. 1847980419847806.
36. Bhagya, L.C., et al., *Structural, optical and photovoltaic properties of V2O5/ZnO and reduced graphene oxide.* Carbon Letters, 2024. **34**(1): p. 13-24.
37. Groeneveld, I., et al., *Parameters that affect the photodegradation of dyes and pigments in solution and on substrate–An overview.* Dyes and Pigments, 2023. **210**: p. 110999.
38. Rahman, S., et al ,.*Research on dye sensitized solar cells: recent advancement toward the various constituents of dye sensitized solar cells for efficiency enhancement and future prospects.* RSC advances, 2023. **13**(28): p. 19508-19529.
39. Seithtanabutara, V., et al., *Potential investigation of combined natural dye pigments extracted from ivy gourd leaves, black glutinous rice and turmeric for dye-sensitised solar cell.* Heliyon, 2023. **9**.(11)